Title

Branching fraction and CP-violation charge asymmetry measurements for B-meson decays to ηK±, ηπ±, η′K, η′π±, ωK, and ωπ±

Journal

Physical Review D, 76(3)

ISSN

2470-0010

Authors

Aubert, B
Bona, M
Boutigny, D
et al.

Publication Date

2007-08-01

DOI

10.1103/physrevd.76.031103

PHYSICAL REVIEW D **76,** 031103(R) (2007)

Branching fraction and *CP*-violation charge asymmetry measurements for *B*-meson decays to $\eta K^{\pm}$, $\eta\pi^{\pm}$, $\eta' K$, $\eta'\pi^{\pm}$, ωK, and $\omega\pi^{\pm}$

B. Aubert,[1] M. Bona,[1] D. Boutigny,[1] Y. Karyotakis,[1] J. P. Lees,[1] V. Poireau,[1] X. Prudent,[1] V. Tisserand,[1] A. Zghiche,[1] J. Garra Tico,[2] E. Grauges,[2] L. Lopez,[3] A. Palano,[3] G. Eigen,[4] B. Stugu,[4] L. Sun,[4] G. S. Abrams,[5] M. Battaglia,[5] D. N. Brown,[5] J. Button-Shafer,[5] R. N. Cahn,[5] Y. Groysman,[5] R. G. Jacobsen,[5] J. A. Kadyk,[5] L. T. Kerth,[5] Yu. G. Kolomensky,[5] G. Kukartsev,[5] D. Lopes Pegna,[5] G. Lynch,[5] L. M. Mir,[5] T. J. Orimoto,[5] M. T. Ronan,[5,*] K. Tackmann,[5] W. A. Wenzel,[5] P. del Amo Sanchez,[6] C. M. Hawkes,[6] A. T. Watson,[6] T. Held,[7] H. Koch,[7] B. Lewandowski,[7] M. Pelizaeus,[7] T. Schroeder,[7] M. Steinke,[7] D. Walker,[8] D. J. Asgeirsson,[9] T. Cuhadar-Donszelmann,[9] B. G. Fulsom,[9] C. Hearty,[9] T. S. Mattison,[9] J. A. McKenna,[9] A. Khan,[10] M. Saleem,[10] L. Teodorescu,[10] V. E. Blinov,[11] A. D. Bukin,[11] V. P. Druzhinin,[11] V. B. Golubev,[11] A. P. Onuchin,[11] S. I. Serednyakov,[11] Yu. I. Skovpen,[11] E. P. Solodov,[11] K. Yu. Todyshev,[11] M. Bondioli,[12] S. Curry,[12] I. Eschrich,[12] D. Kirkby,[12] A. J. Lankford,[12] P. Lund,[12] M. Mandelkern,[12] E. C. Martin,[12] D. P. Stoker,[12] S. Abachi,[13] C. Buchanan,[13] S. D. Foulkes,[14] J. W. Gary,[14] F. Liu,[14] O. Long,[14] B. C. Shen,[14] L. Zhang,[14] H. P. Paar,[15] S. Rahatlou,[15] V. Sharma,[15] J. W. Berryhill,[16] C. Campagnari,[16] A. Cunha,[16] B. Dahmes,[16] T. M. Hong,[16] D. Kovalskyi,[16] J. D. Richman,[16] T. W. Beck,[17] A. M. Eisner,[17] C. J. Flacco,[17] C. A. Heusch,[17] J. Kroseberg,[17] W. S. Lockman,[17] T. Schalk,[17] B. A. Schumm,[17] A. Seiden,[17] M. G. Wilson,[17] L. O. Winstrom,[17] E. Chen,[18] C. H. Cheng,[18] F. Fang,[18] D. G. Hitlin,[18] I. Narsky,[18] T. Piatenko,[18] F. C. Porter,[18] R. Andreassen,[19] G. Mancinelli,[19] B. T. Meadows,[19] K. Mishra,[19] M. D. Sokoloff,[19] F. Blanc,[20] P. C. Bloom,[20] S. Chen,[20] Z. C. Clifton,[20] W. T. Ford,[20] J. F. Hirschauer,[20] A. Kreisel,[20] M. Nagel,[20] U. Nauenberg,[20] A. Olivas,[20] J. G. Smith,[20] K. A. Ulmer,[20] S. R. Wagner,[20] J. Zhang,[20] A. M. Gabareen,[21] A. Soffer,[21] W. H. Toki,[21] R. J. Wilson,[21] F. Winklmeier,[21] D. D. Altenburg,[22] E. Feltresi,[22] A. Hauke,[22] H. Jasper,[22] J. Merkel,[22] A. Petzold,[22] B. Spaan,[22] K. Wacker,[22] V. Klose,[23] M. J. Kobel,[23] H. M. Lacker,[23] W. F. Mader,[23] R. Nogowski,[23] J. Schubert,[23] K. R. Schubert,[23] R. Schwierz,[23] J. E. Sundermann,[23] A. Volk,[23] D. Bernard,[24] G. R. Bonneaud,[24] E. Latour,[24] V. Lombardo,[24] Ch. Thiebaux,[24] M. Verderi,[24] P. J. Clark,[25] W. Gradl,[25] F. Muheim,[25] S. Playfer,[25] A. I. Robertson,[25] Y. Xie,[25] M. Andreotti,[26] D. Bettoni,[26] C. Bozzi,[26] R. Calabrese,[26] A. Cecchi,[26] G. Cibinetto,[26] P. Franchini,[26] E. Luppi,[26] M. Negrini,[26] A. Petrella,[26] L. Piemontese,[26] E. Prencipe,[26] V. Santoro,[26] F. Anulli,[27] R. Baldini-Ferroli,[27] A. Calcaterra,[27] R. de Sangro,[27] G. Finocchiaro,[27] S. Pacetti,[27] P. Patteri,[27] I. M. Peruzzi,[27,†] M. Piccolo,[27] M. Rama,[27] A. Zallo,[27] A. Buzzo,[28] R. Contri,[28] M. Lo Vetere,[28] M. M. Macri,[28] M. R. Monge,[28] S. Passaggio,[28] C. Patrignani,[28] E. Robutti,[28] A. Santroni,[28] S. Tosi,[28] K. S. Chaisanguanthum,[29] M. Morii,[29] J. Wu,[29] R. S. Dubitzky,[30] J. Marks,[30] S. Schenk,[30] U. Uwer,[30] D. J. Bard,[31] P. D. Dauncey,[31] R. L. Flack,[31] J. A. Nash,[31] W. Panduro Vazquez,[31] M. Tibbetts,[31] P. K. Behera,[32] X. Chai,[32] M. J. Charles,[32] U. Mallik,[32] V. Ziegler,[32] J. Cochran,[33] H. B. Crawley,[33] L. Dong,[33] V. Eyges,[33] W. T. Meyer,[33] S. Prell,[33] E. I. Rosenberg,[33] A. E. Rubin,[33] Y. Y. Gao,[34] A. V. Gritsan,[34] Z. J. Guo,[34] C. K. Lae,[34] A. G. Denig,[35] M. Fritsch,[35] G. Schott,[35] N. Arnaud,[36] J. Béquilleux,[36] M. Davier,[36] G. Grosdidier,[36] A. Höcker,[36] V. Lepeltier,[36] F. Le Diberder,[36] A. M. Lutz,[36] S. Pruvot,[36] S. Rodier,[36] P. Roudeau,[36] M. H. Schune,[36] J. Serrano,[36] V. Sordini,[36] A. Stocchi,[36] W. F. Wang,[36] G. Wormser,[36] D. J. Lange,[37] D. M. Wright,[37] I. Bingham,[38] C. A. Chavez,[38] I. J. Forster,[38] J. R. Fry,[38] E. Gabathuler,[38] R. Gamet,[38] D. E. Hutchcroft,[38] D. J. Payne,[38] K. C. Schofield,[38] C. Touramanis,[38] A. J. Bevan,[39] K. A. George,[39] F. Di Lodovico,[39] W. Menges,[39] R. Sacco,[39] G. Cowan,[40] H. U. Flaecher,[40] D. A. Hopkins,[40] S. Paramesvaran,[40] F. Salvatore,[40] A. C. Wren,[40] D. N. Brown,[41] C. L. Davis,[41] J. Allison,[42] N. R. Barlow,[42] R. J. Barlow,[42] Y. M. Chia,[42] C. L. Edgar,[42] G. D. Lafferty,[42] T. J. West,[42] J. I. Yi,[42] J. Anderson,[43] C. Chen,[43] A. Jawahery,[43] D. A. Roberts,[43] G. Simi,[43] J. M. Tuggle,[43] G. Blaylock,[44] C. Dallapiccola,[44] S. S. Hertzbach,[44] X. Li,[44] T. B. Moore,[44] E. Salvati,[44] S. Saremi,[44] R. Cowan,[45] D. Dujmic,[45] P. H. Fisher,[45] K. Koeneke,[45] G. Sciolla,[45] S. J. Sekula,[45] M. Spitznagel,[45] F. Taylor,[45] R. K. Yamamoto,[45] M. Zhao,[45] Y. Zheng,[45] S. E. Mclachlin,[46,*] P. M. Patel,[46] S. H. Robertson,[46] A. Lazzaro,[47] F. Palombo,[47] J. M. Bauer,[48] L. Cremaldi,[48] V. Eschenburg,[48] R. Godang,[48] R. Kroeger,[48] D. A. Sanders,[48] D. J. Summers,[48] H. W. Zhao,[48] S. Brunet,[49] D. Côté,[49] M. Simard,[49] P. Taras,[49] F. B. Viaud,[49] H. Nicholson,[50] G. De Nardo,[51] F. Fabozzi,[51,‡] L. Lista,[51] D. Monorchio,[51] C. Sciacca,[51] M. A. Baak,[52] G. Raven,[52] H. L. Snoek,[52] C. P. Jessop,[53] J. M. LoSecco,[53] G. Benelli,[54] L. A. Corwin,[54] K. Honscheid,[54] H. Kagan,[54] R. Kass,[54] J. P. Morris,[54] A. M. Rahimi,[54] J. J. Regensburger,[54] Q. K. Wong,[54] N. L. Blount,[55] J. Brau,[55] R. Frey,[55] O. Igonkina,[55] J. A. Kolb,[55] M. Lu,[55] R. Rahmat,[55] N. B. Sinev,[55] D. Strom,[55] J. Strube,[55] E. Torrence,[55] N. Gagliardi,[56] A. Gaz,[56] M. Margoni,[56] M. Morandin,[56] A. Pompili,[56] M. Posocco,[56] M. Rotondo,[56] F. Simonetto,[56] R. Stroili,[56] C. Voci,[56] E. Ben-Haim,[57] H. Briand,[57] G. Calderini,[57] J. Chauveau,[57] P. David,[57] L. Del Buono,[57] Ch. de la Vaissière,[57] O. Hamon,[57] Ph. Leruste,[57] J. Malclès,[57] J. Ocariz,[57] A. Perez,[57] L. Gladney,[58] M. Biasini,[59] R. Covarelli,[59] E. Manoni,[59] C. Angelini,[60] G. Batignani,[60] S. Bettarini,[60] M. Carpinelli,[60] R. Cenci,[60]

A. Cervelli,[60] F. Forti,[60] M. A. Giorgi,[60] A. Lusiani,[60] G. Marchiori,[60] M. A. Mazur,[60] M. Morganti,[60] N. Neri,[60] E. Paoloni,[60] G. Rizzo,[60] J. J. Walsh,[60] M. Haire,[61] J. Biesiada,[62] P. Elmer,[62] Y. P. Lau,[62] C. Lu,[62] J. Olsen,[62] A. J. S. Smith,[62] A. V. Telnov,[62] E. Baracchini,[63] F. Bellini,[63] G. Cavoto,[63] A. D'Orazio,[63] D. del Re,[63] E. Di Marco,[63] R. Faccini,[63] F. Ferrarotto,[63] F. Ferroni,[63] M. Gaspero,[63] P. D. Jackson,[63] L. Li Gioi,[63] M. A. Mazzoni,[63] S. Morganti,[63] G. Piredda,[63] F. Polci,[63] F. Renga,[63] C. Voena,[63] M. Ebert,[64] T. Hartmann,[64] H. Schröder,[64] R. Waldi,[64] T. Adye,[65] G. Castelli,[65] B. Franek,[65] E. O. Olaiya,[65] S. Ricciardi,[65] W. Roethel,[65] F. F. Wilson,[65] R. Aleksan,[66] S. Emery,[66] M. Escalier,[66] A. Gaidot,[66] S. F. Ganzhur,[66] G. Hamel de Monchenault,[66] W. Kozanecki,[66] G. Vasseur,[66] Ch. Yèche,[66] M. Zito,[66] X. R. Chen,[67] H. Liu,[67] W. Park,[67] M. V. Purohit,[67] J. R. Wilson,[67] M. T. Allen,[68] D. Aston,[68] R. Bartoldus,[68] P. Bechtle,[68] N. Berger,[68] R. Claus,[68] J. P. Coleman,[68] M. R. Convery,[68] J. C. Dingfelder,[68] J. Dorfan,[68] G. P. Dubois-Felsmann,[68] W. Dunwoodie,[68] R. C. Field,[68] T. Glanzman,[68] S. J. Gowdy,[68] M. T. Graham,[68] P. Grenier,[68] C. Hast,[68] T. Hryn'ova,[68] W. R. Innes,[68] J. Kaminski,[68] M. H. Kelsey,[68] H. Kim,[68] P. Kim,[68] M. L. Kocian,[68] D. W. G. S. Leith,[68] S. Li,[68] S. Luitz,[68] V. Luth,[68] H. L. Lynch,[68] D. B. MacFarlane,[68] H. Marsiske,[68] R. Messner,[68] D. R. Muller,[68] C. P. O'Grady,[68] I. Ofte,[68] A. Perazzo,[68] M. Perl,[68] T. Pulliam,[68] B. N. Ratcliff,[68] A. Roodman,[68] A. A. Salnikov,[68] R. H. Schindler,[68] J. Schwiening,[68] A. Snyder,[68] J. Stelzer,[68] D. Su,[68] M. K. Sullivan,[68] K. Suzuki,[68] S. K. Swain,[68] J. M. Thompson,[68] J. Va'vra,[68] N. van Bakel,[68] A. P. Wagner,[68] M. Weaver,[68] W. J. Wisniewski,[68] M. Wittgen,[68] D. H. Wright,[68] A. K. Yarritu,[68] K. Yi,[68] C. C. Young,[68] P. R. Burchat,[69] A. J. Edwards,[69] S. A. Majewski,[69] B. A. Petersen,[69] L. Wilden,[69] S. Ahmed,[70] M. S. Alam,[70] R. Bula,[70] J. A. Ernst,[70] V. Jain,[70] B. Pan,[70] M. A. Saeed,[70] F. R. Wappler,[70] S. B. Zain,[70] W. Bugg,[71] M. Krishnamurthy,[71] S. M. Spanier,[71] R. Eckmann,[72] J. L. Ritchie,[72] A. M. Ruland,[72] C. J. Schilling,[72] R. F. Schwitters,[72] J. M. Izen,[73] X. C. Lou,[73] S. Ye,[73] F. Bianchi,[74] F. Gallo,[74] D. Gamba,[74] M. Pelliccioni,[74] M. Bomben,[75] L. Bosisio,[75] C. Cartaro,[75] F. Cossutti,[75] G. Della Ricca,[75] L. Lanceri,[75] L. Vitale,[75] V. Azzolini,[76] N. Lopez-March,[76] F. Martinez-Vidal,[76,§] D. A. Milanes,[76] A. Oyanguren,[76] J. Albert,[77] Sw. Banerjee,[77] B. Bhuyan,[77] K. Hamano,[77] R. Kowalewski,[77] I. M. Nugent,[77] J. M. Roney,[77] R. J. Sobie,[77] P. F. Harrison,[78] J. Ilic,[78] T. E. Latham,[78] G. B. Mohanty,[78] M. Pappagallo,[78,‖] H. R. Band,[79] X. Chen,[79] S. Dasu,[79] K. T. Flood,[79] J. J. Hollar,[79] P. E. Kutter,[79] Y. Pan,[79] M. Pierini,[79] R. Prepost,[79] S. L. Wu,[79] and H. Neal[80]

(*BABAR* Collaboration)

[1]*Laboratoire de Physique des Particules, IN2P3/CNRS et Université de Savoie, F-74941 Annecy-Le-Vieux, France*
[2]*Universitat de Barcelona, Facultat de Fisica, Departament ECM, E-08028 Barcelona, Spain*
[3]*Università di Bari, Dipartimento di Fisica and INFN, I-70126 Bari, Italy*
[4]*University of Bergen, Institute of Physics, N-5007 Bergen, Norway*
[5]*Lawrence Berkeley National Laboratory and University of California, Berkeley, California 94720, USA*
[6]*University of Birmingham, Birmingham, B15 2TT, United Kingdom*
[7]*Ruhr Universität Bochum, Institut für Experimentalphysik 1, D-44780 Bochum, Germany*
[8]*University of Bristol, Bristol BS8 1TL, United Kingdom*
[9]*University of British Columbia, Vancouver, British Columbia, Canada V6T 1Z1*
[10]*Brunel University, Uxbridge, Middlesex UB8 3PH, United Kingdom*
[11]*Budker Institute of Nuclear Physics, Novosibirsk 630090, Russia*
[12]*University of California at Irvine, Irvine, California 92697, USA*
[13]*University of California at Los Angeles, Los Angeles, California 90024, USA*
[14]*University of California at Riverside, Riverside, California 92521, USA*
[15]*University of California at San Diego, La Jolla, California 92093, USA*
[16]*University of California at Santa Barbara, Santa Barbara, California 93106, USA*
[17]*University of California at Santa Cruz, Institute for Particle Physics, Santa Cruz, California 95064, USA*
[18]*California Institute of Technology, Pasadena, California 91125, USA*
[19]*University of Cincinnati, Cincinnati, Ohio 45221, USA*
[20]*University of Colorado, Boulder, Colorado 80309, USA*
[21]*Colorado State University, Fort Collins, Colorado 80523, USA*
[22]*Universität Dortmund, Institut für Physik, D-44221 Dortmund, Germany*
[23]*Technische Universität Dresden, Institut für Kern-und Teilchenphysik, D-01062 Dresden, Germany*
[24]*Laboratoire Leprince-Ringuet, CNRS/IN2P3, Ecole Polytechnique, F-91128 Palaiseau, France*
[25]*University of Edinburgh, Edinburgh EH9 3JZ, United Kingdom*
[26]*Università di Ferrara, Dipartimento di Fisica and INFN, I-44100 Ferrara, Italy*
[27]*Laboratori Nazionali di Frascati dell'INFN, I-00044 Frascati, Italy*
[28]*Università di Genova, Dipartimento di Fisica and INFN, I-16146 Genova, Italy*
[29]*Harvard University, Cambridge, Massachusetts 02138, USA*

[30]*Universität Heidelberg, Physikalisches Institut, Philosophenweg 12, D-69120 Heidelberg, Germany*
[31]*Imperial College London, London, SW7 2AZ, United Kingdom*
[32]*University of Iowa, Iowa City, Iowa 52242, USA*
[33]*Iowa State University, Ames, Iowa 50011-3160, USA*
[34]*Johns Hopkins University, Baltimore, Maryland 21218, USA*
[35]*Universität Karlsruhe, Institut für Experimentelle Kernphysik, D-76021 Karlsruhe, Germany*
[36]*Laboratoire de l'Accélérateur Linéaire, IN2P3/CNRS et Université Paris-Sud 11, Centre Scientifique d'Orsay, B. P. 34, F-91898 ORSAY Cedex, France*
[37]*Lawrence Livermore National Laboratory, Livermore, California 94550, USA*
[38]*University of Liverpool, Liverpool L69 7ZE, United Kingdom*
[39]*Queen Mary, University of London, E1 4NS, United Kingdom*
[40]*University of London, Royal Holloway and Bedford New College, Egham, Surrey TW20 0EX, United Kingdom*
[41]*University of Louisville, Louisville, Kentucky 40292, USA*
[42]*University of Manchester, Manchester M13 9PL, United Kingdom*
[43]*University of Maryland, College Park, Maryland 20742, USA*
[44]*University of Massachusetts, Amherst, Massachusetts 01003, USA*
[45]*Massachusetts Institute of Technology, Laboratory for Nuclear Science, Cambridge, Massachusetts 02139, USA*
[46]*McGill University, Montréal, Québec, Canada H3A 2T8*
[47]*Università di Milano, Dipartimento di Fisica and INFN, I-20133 Milano, Italy*
[48]*University of Mississippi, University, Mississippi 38677, USA*
[49]*Université de Montréal, Physique des Particules, Montréal, Québec, Canada H3C 3J7*
[50]*Mount Holyoke College, South Hadley, Massachusetts 01075, USA*
[51]*Università di Napoli Federico II, Dipartimento di Scienze Fisiche and INFN, I-80126, Napoli, Italy*
[52]*NIKHEF, National Institute for Nuclear Physics and High Energy Physics, NL-1009 DB Amsterdam, The Netherlands*
[53]*University of Notre Dame, Notre Dame, Indiana 46556, USA*
[54]*Ohio State University, Columbus, Ohio 43210, USA*
[55]*University of Oregon, Eugene, Oregon 97403, USA*
[56]*Università di Padova, Dipartimento di Fisica and INFN, I-35131 Padova, Italy*
[57]*Laboratoire de Physique Nucléaire et de Hautes Energies, IN2P3/CNRS, Université Pierre et Marie Curie-Paris6, Université Denis Diderot-Paris7, F-75252 Paris, France*
[58]*University of Pennsylvania, Philadelphia, Pennsylvania 19104, USA*
[59]*Università di Perugia, Dipartimento di Fisica and INFN, I-06100 Perugia, Italy*
[60]*Università di Pisa, Dipartimento di Fisica, Scuola Normale Superiore and INFN, I-56127 Pisa, Italy*
[61]*Prairie View A&M University, Prairie View, Texas 77446, USA*
[62]*Princeton University, Princeton, New Jersey 08544, USA*
[63]*Università di Roma La Sapienza, Dipartimento di Fisica and INFN, I-00185 Roma, Italy*
[64]*Universität Rostock, D-18051 Rostock, Germany*
[65]*Rutherford Appleton Laboratory, Chilton, Didcot, Oxon, OX11 0QX, United Kingdom*
[66]*DSM/Dapnia, CEA/Saclay, F-91191 Gif-sur-Yvette, France*
[67]*University of South Carolina, Columbia, South Carolina 29208, USA*
[68]*Stanford Linear Accelerator Center, Stanford, California 94309, USA*
[69]*Stanford University, Stanford, California 94305-4060, USA*
[70]*State University of New York, Albany, New York 12222, USA*
[71]*University of Tennessee, Knoxville, Tennessee 37996, USA*
[72]*University of Texas at Austin, Austin, Texas 78712, USA*
[73]*University of Texas at Dallas, Richardson, Texas 75083, USA*
[74]*Università di Torino, Dipartimento di Fisica Sperimentale and INFN, I-10125 Torino, Italy*
[75]*Università di Trieste, Dipartimento di Fisica and INFN, I-34127 Trieste, Italy*
[76]*IFIC, Universitat de Valencia-CSIC, E-46071 Valencia, Spain*
[77]*University of Victoria, Victoria, British Columbia, Canada V8W 3P6*
[78]*Department of Physics, University of Warwick, Coventry CV4 7AL, United Kingdom*
[79]*University of Wisconsin, Madison, Wisconsin 53706, USA*
[80]*Yale University, New Haven, Connecticut 06511, USA*
(Received 26 June 2007; published 28 August 2007)

[*]Deceased.
[†]Also with Università di Perugia, Dipartimento di Fisica, Perugia, Italy.
[‡]Also with Università della Basilicata, Potenza, Italy.
[§]Also with Universitat de Barcelona, Facultat de Fisica, Departament ECM, E-08028 Barcelona, Spain.
[‖]Also with IPPP, Physics Department, Durham University, Durham DH1 3LE, United Kingdom.

We present measurements of the branching fractions for B^0-meson decays to $\eta' K^0$ and ωK^0, and of the branching fractions and CP-violation charge asymmetries for B^+-meson decays to $\eta\pi^+$, ηK^+, $\eta'\pi^+$, $\eta' K^+$, $\omega\pi^+$, and ωK^+. The data, collected with the *BABAR* detector at the Stanford Linear Accelerator Center, represent 383×10^6 $B\bar{B}$ pairs produced in e^+e^- annihilation. The measurements agree with previous results; we find no evidence for direct CP violation.

DOI: 10.1103/PhysRevD.76.031103 PACS numbers: 13.25.Hw, 11.30.Er, 12.15.Hh, 12.39.St

Charmless B decays are becoming increasingly useful to test the accuracy of theoretical estimation methods, such as those based on QCD factorization [1–3] or flavor SU(3) symmetry [4–6]. In this paper we present measurements of branching fractions and, where applicable, charge asymmetries, for eight charmless B decays (and their charge conjugates, implied throughout the paper): $B^+ \to \eta\pi^+$, $B^+ \to \eta K^+$, $B^+ \to \eta'\pi^+$, $B^+ \to \eta' K^+$, $B^0 \to \eta' K^0$, $B^+ \to \omega\pi^+$, $B^+ \to \omega K^+$, and $B^0 \to \omega K^0$. The results presented here represent improvement in precision over previous measurements of these quantities by *BABAR* [7–9], Belle [10–12], and CLEO [13]. We previously reported a branching fraction limit for $B^0 \to \eta K^0$ [14], and CP asymmetries for $B^0 \to \eta' K^0$ and $B^0 \to \omega K^0$ [9,15].

Charmless B decays with kaons are usually expected to be dominated by $b \to s$ loop ("penguin") amplitudes, while $b \to u$ tree amplitudes typically dominate for the decays with pions. However, the $B \to \eta K$ decays are especially interesting since they are suppressed relative to the abundant $B \to \eta' K$ decays due to destructive interference between two penguin amplitudes [16]. The Cabibbo-Kobayashi-Maskawa (CKM)-suppressed $b \to u$ tree amplitudes may interfere significantly with $b \to s$ penguin amplitudes of similar magnitudes, possibly leading to large direct CP violation in $B^+ \to \eta\pi^+$ and $B^+ \to \eta'\pi^+$ [17]; numerical estimates are available in a few cases [2–4,18]. We search for such direct CP violation by measuring the charge asymmetry $\mathcal{A}_{\rm ch} \equiv (\Gamma^- - \Gamma^+)/(\Gamma^- + \Gamma^+)$ in the rates $\Gamma^\pm = \Gamma(B^\pm \to f^\pm)$ for each charged final state $f^\pm$.

Finally, phenomenological fits to the branching fractions and charge asymmetries of charmless B decays can be used to understand the relative importance of tree and penguin contributions and may provide sensitivity to the CKM angle γ [4–6,19], or to the effect of non–standard-model heavy particles in the loops [20].

The results presented here are based on data collected with the *BABAR* detector [21] at the PEP-II e^+e^- collider [22] located at the Stanford Linear Accelerator Center. An integrated luminosity of 347 fb^{-1}, corresponding to 383×10^6 $B\bar{B}$ pairs, was recorded at the $\Upsilon(4S)$ resonance (center-of-mass energy $\sqrt{s} = 10.58$ GeV).

Charged particles from the e^+e^- interactions are detected, and their momenta measured, by a combination of five layers of double-sided silicon microstrip detectors and a 40-layer drift chamber, both operating in the 1.5 T magnetic field of a superconducting solenoid. Photons and electrons are identified with a CsI(Tl) electromagnetic calorimeter (EMC). Further charged particle identification (PID) is provided by the average energy loss (dE/dx) in the tracking devices and by an internally reflecting ring imaging Cherenkov detector (DIRC) covering the central region.

We establish the event selection criteria with the aid of a detailed Monte Carlo (MC) simulation of the B production and decay sequences, and of the detector response [23]. These criteria are designed to retain signal events with high efficiency. When applied to the data, they result in a sample much larger than the expected signal, but with well-characterized backgrounds. We extract the signal yields from this sample with a maximum likelihood (ML) fit.

The B-daughter candidates are reconstructed through their decays $\pi^0 \to \gamma\gamma$, $K^0 \to K^0_S \to \pi^+\pi^-$, $\omega \to \pi^+\pi^-\pi^0$, $\eta \to \gamma\gamma$ ($\eta_{\gamma\gamma}$), $\eta \to \pi^+\pi^-\pi^0$ ($\eta_{3\pi}$), $\eta' \to \eta_{\gamma\gamma}\pi^+\pi^-$ ($\eta'_{\eta\pi\pi}$), and $\eta' \to \rho^0\gamma$ ($\eta'_{\rho\gamma}$), where $\rho^0 \to \pi^+\pi^-$. The invariant mass of these particles' final states are required to lie within about 2 standard deviations of the nominal mass [24] unless the mass is an observable in the ML fit, in which case we accept a wider range. For a K^0_S candidate we require a successful fit of the decay vertex with the flight direction constrained to the pion pair momentum direction, yielding a flight length greater than 3 times its uncertainty. Secondary charged pions in η', η, and ω candidates are rejected if classified as protons, kaons, or electrons by their DIRC, dE/dx, and EMC PID signatures. For the primary charged track in B^+ decays we define the PID variables S_π and S_K as the number of standard deviations between the measured DIRC Cherenkov angle and that expected for pions and kaons, respectively. We include these observables in the ML fits to distinguish between primary π and K. For $B^+ \to \eta' K^+$ the backgrounds, including cross feed from the pion channel, are small. For this mode we perform a dedicated fit with less restrictive continuum background rejection (see below), and $S_K < 2$ to exclude pions (and lighter particles).

We reconstruct the B-meson candidate by combining the four-momenta of a pair of daughter mesons with a vertex constraint if the ultimate final state includes at least two charged particles. Since the natural widths of the η, η', and π^0 are much smaller than the resolution, we also constrain their masses to nominal values [24] in the fit of the B candidate. From the kinematics of $\Upsilon(4S)$ decay we determine the energy-substituted mass $m_{\rm ES} = \sqrt{\frac{1}{4}s - \mathbf{p}_B^2}$ and energy difference $\Delta E = E_B - \frac{1}{2}\sqrt{s}$, where $(E_B, \mathbf{p}_B)$ is the B-meson four-momentum vector, and all values are ex-

pressed in the $\Upsilon(4S)$ frame. The resolution in $m_{\rm ES}$ is 3.0 MeV and in ΔE is 24–50 MeV, depending on the decay mode. We require $5.25 < m_{\rm ES} < 5.29$ GeV and $|\Delta E| < 0.2$ GeV.

Backgrounds arise primarily from random combinations of particles in continuum $e^+e^- \to q\bar{q}$ events ($q = u, d, s, c$). We reduce these with requirements on the angle $\theta_{\rm T}$ between the thrust axis of the B candidate in the $\Upsilon(4S)$ frame and that of the rest of the charged tracks and neutral calorimeter clusters in the event. The distribution is sharply peaked near $|\cos\theta_{\rm T}| = 1$ for $q\bar{q}$ jet pairs, and nearly uniform for B-meson decays. We require $|\cos\theta_{\rm T}| < 0.90$ (< 0.65 for $\eta'_{\rho\gamma}\pi^+$, <0.80 for $\omega\pi^+$ and ωK^+), which optimizes the expected signal yield relative to its background-dominated statistical error. In the ML fit we discriminate further against $q\bar{q}$ background with a Fisher discriminant $\mathcal{F}$ that combines several variables which characterize the energy flow in the event [25]. It provides about 1 standard deviation of separation between B decay events and $q\bar{q}$ background [see Fig. 1(c)].

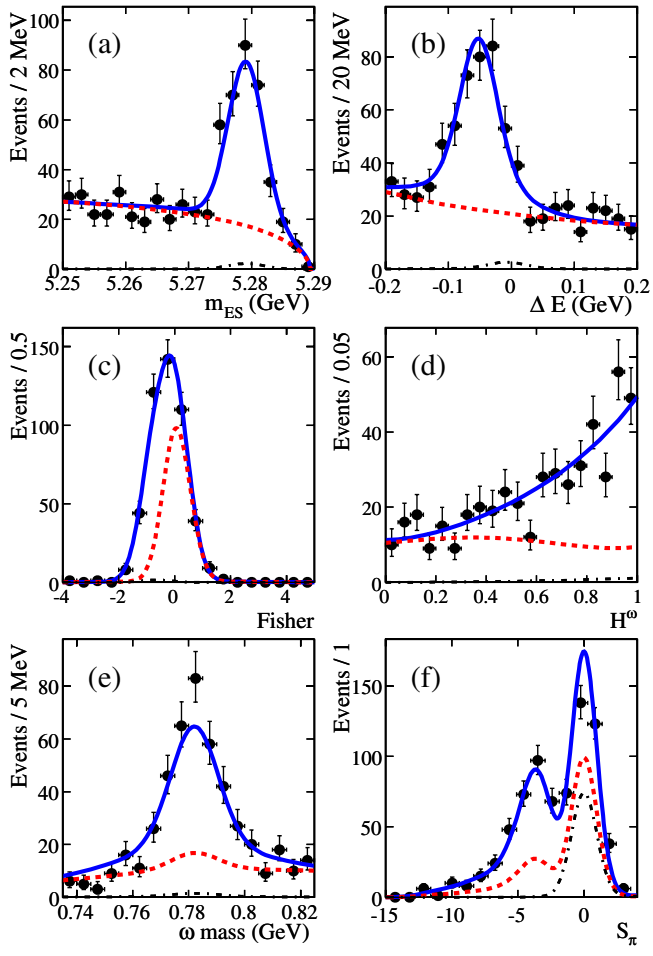

FIG. 1 (color online). Plots of signal-enhanced subsets of the data distribution for $B^+ \to \omega K^+$ projected on each of the fit variables: (a) $m_{\rm ES}$, (b) ΔE, (c) $\mathcal{F}$, (d) $\mathcal{H}^\omega$, (e) ω mass, and (f) S_π. Points with errors represent the data, solid curves the full fit functions, dashed curves the sum of the background functions, and dot-dashed curves the signal from $B^+ \to \omega\pi^+$. The variable ΔE is computed with the pion mass.

We also impose restrictions on resonance decay angles to exclude the most asymmetric decays where soft-particle backgrounds accumulate and the acceptance changes rapidly. We define the decay angle $\theta^r_{\rm dec}$ for a meson r that decays to two particles as the angle between the momenta of a daughter particle and the meson's parent, measured in the meson's rest frame. We define $\mathcal{H}^r \equiv \cos\theta^r_{\rm dec}$ and require $|\mathcal{H}^{\rho^0}| < 0.9$ for $B \to \eta'_{\rho\gamma}K$ and $|\mathcal{H}^{\rho^0}| < 0.7$ for $B^+ \to \eta'_{\rho\gamma}\pi^+$. For the three-body $\omega \to 3\pi$ mode the direction for the decay is the normal to the decay plane, and we include $\mathcal{H}^\omega$ as an observable in the ML fit.

The average number of candidates found per selected event is in the range 1.05 to 1.13, depending on the final state. We choose the candidate with the daughter resonance mass closest to the nominal value. From the simulation we find that this algorithm selects the correct-combination candidate in about two-thirds of the events containing multiple candidates, and that it induces negligible bias in the ML fits.

We obtain yields for each channel from an extended maximum likelihood fit with the input observables ΔE, $m_{\rm ES}$, $\mathcal{F}$, m_r (the invariant mass of the η, η', or ω candidate), and, for charged decays other than $B^+ \to \eta' K^+$, the PID variables S_π and S_K. The selected data sample sizes are given in the second column of Table I. Besides the signal events they contain $q\bar{q}$ (dominant) and $B\bar{B}$ with $b \to c$ combinatorial background, and a fraction of background from other charmless $B\bar{B}$ modes, which we estimate from the simulation to be less than 2% of the total fit sample. The latter events have ultimate final states different from the signal, but with similar kinematics so that broad peaks near those of the signal appear in some observables, requiring a separate component in the probability density function (PDF). The yield of this component is free in the fit for all cases except $B^0 \to \omega K^0_S$, where the fit stability requires fixing the yield to the expectation from MC. The likelihood function is

$$\mathcal{L} = \exp\Big(-\sum_{j,k} Y_{jk}\Big)\prod_i^N \sum_{j,k} Y_{jk}\mathcal{P}_j(m_{\rm ES}{}^i)\mathcal{P}_j(\mathcal{F}^i)\mathcal{P}_j(\Delta E^i_k) \times [\mathcal{P}_j(S^i_k)\mathcal{P}_j(m^i_r)\mathcal{P}_j(\mathcal{H}^i_r)], \quad (1)$$

where N is the number of events in the sample, and for each component j (signal, combinatorial background, or charmless $B\bar{B}$ background) and flavor k (primary K^+ or π^+), Y_{jk} is the yield of events and $\mathcal{P}_j(x^i_k)$ the PDF for observable x_k in event i. Some factors in [ ] are omitted for some modes. The flavor-dependent factors $\mathcal{P}_j(\Delta E^i_k)$ and $\mathcal{P}_j(S^i_k)$ take common functional forms for the pion or kaon, e.g., $F_j(\Delta E^i_\pi)$ or $F_j(\Delta E^i_K = \Delta E^i_\pi + \delta\Delta E(\mathbf{p}^i))$, where $\mathbf{p}$ is the primary-track momentum; S^i_k is treated similarly. For the modes $B \to \eta'_{\eta\pi\pi}K$ we found no need for the $B\bar{B}$ back-

TABLE I. Number of events N in the sample, fitted signal yield Y_S, and measured bias (to be subtracted from Y_S) in events (ev.), detection efficiency ϵ, daughter branching fraction product ($\prod \mathcal{B}_i$), and measured branching fraction $\mathcal{B}$ and charge asymmetry $\mathcal{A}_{\rm ch}$ with statistical errors for each decay chain, and for the combined measurements the branching fraction and charge asymmetry with statistical and systematic error. The number of produced $B\bar{B}$ pairs is given in the text.

Mode	N (ev.)	Y_S (ev.)	Bias (ev.)	ϵ (%)	$\prod \mathcal{B}_i$ (%)	$\mathcal{B}$ (10^{-6})	$\mathcal{A}_{\rm ch}$
$\boldsymbol{\eta\pi^+}$						**5.0±0.5±0.3**	**−0.08±0.10±0.01**
$\eta_{\gamma\gamma}\pi^+$	44 883	258^{+30}_{-29}	6 ± 3	34.1	39.4	4.9 ± 0.6	−0.05 ± 0.12
$\eta_{3\pi}\pi^+$	22 333	115^{+20}_{-19}	6 ± 3	23.8	22.6	5.5 ± 1.0	−0.13 ± 0.18
$\boldsymbol{\eta K^+}$						**3.7±0.4±0.1**	**−0.22±0.11±0.01**
$\eta_{\gamma\gamma}K^+$	44 883	197^{+25}_{-24}	6 ± 3	32.7	39.4	3.9 ± 0.5	−0.25 ± 0.13
$\eta_{3\pi}K^+$	22 333	71^{+16}_{-15}	4 ± 2	23.2	22.6	3.3 ± 0.8	−0.15 ± 0.23
$\boldsymbol{\eta'\pi^+}$						**3.9±0.7±0.3**	**0.21±0.17±0.01**
$\eta'_{\eta\pi\pi}\pi^+$	16 879	88^{+16}_{-15}	14 ± 3	27.2	17.5	4.0 ± 0.9	0.14 ± 0.20
$\eta'_{\rho\gamma}\pi^+$	35 523	97^{+23}_{-22}	23 ± 7	18.4	29.4	3.6 ± 1.1	0.35 ± 0.30
$\boldsymbol{\eta'K^+}$						**70.0±1.5±2.8**	**0.010±0.022±0.006**
$\eta'_{\eta\pi\pi}K^+$	3170	1060 ± 35	0 ± 1	23.2	17.5	68.2 ± 2.3	−0.005 ± 0.033
$\eta'_{\rho\gamma}K^+$	79 501	2405 ± 69	31 ± 16	29.2	29.4	72.2 ± 2.1	0.022 ± 0.028
$\boldsymbol{\eta'K^0}$						**66.6±2.6±2.8**	(see [15])
$\eta'_{\eta\pi\pi}K^0$	1100	329 ± 20	3 ± 1	23.2	6.1	60.7 ± 3.7	···
$\eta'_{\rho\gamma}K^0$	19 927	831 ± 38	35 ± 17	28.0	10.2	72.8 ± 3.5	···
$\boldsymbol{\omega\pi^+}$	76 735	516 ± 38	44 ± 22	20.5	89.1	**6.7±0.5±0.4**	**−0.02±0.08±0.01**
$\boldsymbol{\omega K^+}$	76 735	457 ± 32	29 ± 15	20.0	89.1	**6.3±0.5±0.3**	**−0.01±0.07±0.01**
$\boldsymbol{\omega K^0}$	15 914	146 ± 18	10 ± 5	21.2	30.8	**5.4±0.8±0.3**	(see [9])

ground component. The factored form of the PDF indicated in Eq. (1) is a good approximation, particularly for the $q\bar{q}$ component, since correlations among observables

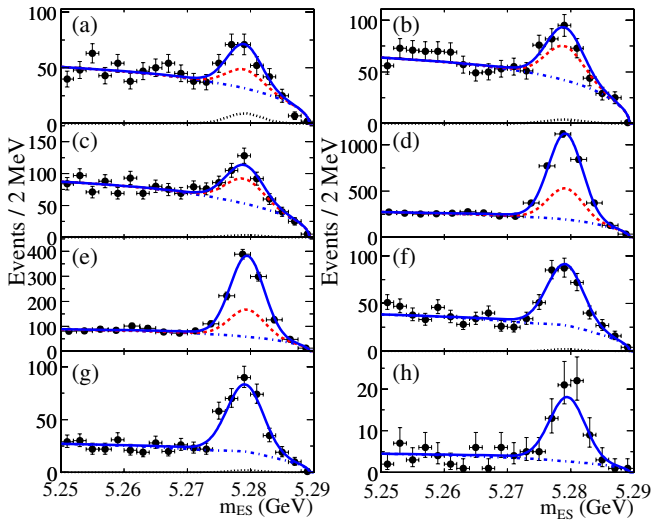

FIG. 2 (color online). Plots of signal-enhanced subsets of the data distributions projected onto $m_{\rm ES}$ for the decays: (a) $B^+ \to \eta\pi^+$, (b) $B^+ \to \eta K^+$, (c) $B^+ \to \eta'\pi^+$, (d) $B^+ \to \eta' K^+$, (e) $B^0 \to \eta' K^0$, (f) $B^+ \to \omega\pi^+$, (g) $B^+ \to \omega K^+$, and (h) $B^0 \to \omega K^0$. The solid line represents the result of the fit, and the dot-dashed line the background contribution. The dashed line gives the sum of background and the $\eta_{3\pi}$ [(a), (b)] or $\eta'_{\eta\pi\pi}$ [(c)–(e)] component of the signal. The dotted line shows the K or π cross-feed component, where applicable.

measured in the data are typically a few percent or less. Distortions of the fit results caused by our approximations are measured in simulation and included in the bias corrections and systematic errors discussed below.

We determine the PDFs for the signal and $B\bar{B}$ background components from fits to MC samples. We calibrate the resolutions in ΔE and $m_{\rm ES}$ with large data control samples of B decays to charmed final states of similar topology [e.g. $B \to D(K\pi\pi)\pi$]. We develop PDFs for the combinatorial background with fits to the data from which the signal region ($5.27\ {\rm GeV} < m_{\rm ES} < 5.29\ {\rm GeV}$ and $|\Delta E| < 0.1\ {\rm GeV}$) has been excluded.

We use the following functional forms for the PDFs: the sum of two Gaussians for $\mathcal{P}_{\rm sig}(m_{\rm ES})$, $\mathcal{P}_{{\rm sig},B\bar{B}}(\Delta E)$, and the sharper structures in $\mathcal{P}_{B\bar{B}}(m_{\rm ES})$ and $\mathcal{P}_j(m_r)$; linear or quadratic dependences for combinatorial components of $\mathcal{P}_{B\bar{B},q\bar{q}}(m_r)$ and for $\mathcal{P}_{q\bar{q}}(\Delta E)$; and a Gaussian function with separate low- and high-side width parameters for $\mathcal{P}_j(\mathcal{F})$. The $q\bar{q}$ background in $m_{\rm ES}$ is described by the threshold function $x\sqrt{1-x^2}\exp[-\xi(1-x^2)]$, with $x \equiv 2m_{\rm ES}/\sqrt{s}$ and parameter ξ. These functions are discussed in more detail in [25], and some of them are illustrated in Fig. 1.

We allow the parameters most important for the determination of the background PDFs to vary in the fit, along with the yields for all components, and for charged modes the signal and $q\bar{q}$ background charge asymmetries. Specifically, the free background parameters are most or all of the following, depending on the decay mode: ξ for $m_{\rm ES}$, linear and quadratic coefficients for ΔE, area and slope of the combinatorial component for m_r, and the

mean, width, and width difference parameters for $\mathcal{F}$. Results for the signal yields are presented in the third column of Table I for each sample.

We validate the fitting procedure by applying it to ensembles of simulated $q\bar{q}$ experiments drawn from the PDF into which we have embedded the expected number of signal and $B\bar{B}$ background events randomly extracted from the fully simulated MC samples. Biases obtained by this procedure with inputs that reproduce the yields found in the data are reported in the fourth column of Table I.

In Fig. 1 we show, as a representative of the fits, the projections of the PDF and data for the $B^+ \to \omega K^+$ fit, and in Fig. 2 projections onto $m_{\rm ES}$ for each of the eight decays, with submodes combined. The data plotted are subsamples enriched in signal with a threshold requirement on the ratio of signal to total likelihood (computed without the plotted variable) that retains 35%–80% of the signal, depending on the mode.

We determine the reconstruction efficiencies as the ratio of reconstructed and accepted events in simulation to the number generated. We compute the branching fraction for each channel by subtracting the fit bias from the measured yield, and dividing the result by the efficiency (including secondary branching fractions) and the number of produced $B\bar{B}$ pairs [25]. We assume equal decay rates of the $\Upsilon(4S)$ to B^+B^- and $B^0\bar{B}^0$. Table I gives the numbers pertinent to these computations. The statistical error on the signal yield or branching fraction is taken as the change in the central value when the quantity $-2\ln\mathcal{L}$ increases by one unit from its minimum value.

We combine results where we have multiple decay channels by adding the functions $-2\ln\{[\mathcal{L}(\mathcal{B})/\mathcal{L}(\mathcal{B}_0)] \otimes G(\sigma')\}$, where $\mathcal{B}_0$ is the central value from the fit for each decay channel, and $\otimes G$ denotes convolution with a Gaussian function to include the systematic error σ' discussed below. We give the resulting final branching fractions for each mode in Table I.

Systematic uncertainties on the branching fractions arise from the PDFs, $B\bar{B}$ backgrounds, fit bias, and efficiency. PDF uncertainties not already accounted for by free parameters in the fit are estimated from the consistency of fits to MC and data in control modes. Varying the signal-PDF parameters within these errors, we estimate yield uncertainties of 0.4%–2.2%, depending on the mode. For the $B\bar{B}$ backgrounds we vary the input branching fractions within their uncertainties for the modes that contribute most to the selected sample. The resulting changes in the signal yield are taken in quadrature and scaled to the total of all modes to determine the systematic uncertainty. For the $\eta'_{\eta\pi\pi}K$ modes, where no $B\bar{B}$ component is used, we use 10% of the expected $B\bar{B}$ background in the sample, as this is the typical correlation with the signal yield. For ωK^0_S where the $B\bar{B}$ yield is fixed, we take as a systematic uncertainty the average change in the signal yield when the $B\bar{B}$ yield is varied between zero and twice the nominal value. The uncertainty of the bias (Table I) is a quadrature sum of its components: the statistical uncertainty from the simulated experiments, and half of the corrections attributable to correlations omitted from the signal and $B\bar{B}$ background models, and to PID of the primary charged track. The primary-track PID correction is significant only for misidentified kaons from $B^+ \to \eta' K^+$ in the $B^+ \to \eta'\pi^+$ channels.

Uncertainties in our knowledge of the efficiency, found from auxiliary studies, include $0.5\% \times N_t$ and $1.5\% \times N_\gamma$, where N_t and N_γ are the number of tracks and photons, respectively, in the B candidate. The uncertainty in the total number of $B\bar{B}$ pairs in the data sample is 1.1%. Published data [24] provide the uncertainties in the B-daughter product branching fractions (0.7%–3.2%). The uncertainties in the efficiency from the event selection are below 0.5%.

For the measurements of $\mathcal{A}_{\rm ch}$, biases arise, in principle, from charge-dependent effects in the track reconstruction or particle identification, or from imperfect modeling of the interactions with material in the detector. We study these by comparing this effect in MC for the signal, $q\bar{q}$ background in the data, and control samples mentioned previously. We apply corrections, and assign systematic errors, to $\mathcal{A}_{\rm ch}$ equal to -0.010 ± 0.005 for modes with a primary kaon and 0.000 ± 0.005 for those with a primary pion. We apply an additional correction with uncertainty for dilution of the $\mathcal{A}_{\rm ch}$ measurement associated with the yield bias, which is significant only for $B^+ \to \eta'_{\eta\pi\pi}\pi^+$. This is obtained from the same MC studies that are used to estimate the yield bias.

After combining the measurements, we obtain for the branching fractions

$$\mathcal{B}(B^+ \to \eta\pi^+) = (5.0 \pm 0.5 \pm 0.3) \times 10^{-6},$$
$$\mathcal{B}(B^+ \to \eta K^+) = (3.7 \pm 0.4 \pm 0.1) \times 10^{-6},$$
$$\mathcal{B}(B^+ \to \eta'\pi^+) = (3.9 \pm 0.7 \pm 0.3) \times 10^{-6},$$
$$\mathcal{B}(B^+ \to \eta' K^+) = (70.0 \pm 1.5 \pm 2.8) \times 10^{-6},$$
$$\mathcal{B}(B^0 \to \eta' K^0) = (66.6 \pm 2.6 \pm 2.8) \times 10^{-6},$$
$$\mathcal{B}(B^+ \to \omega\pi^+) = (6.7 \pm 0.5 \pm 0.4) \times 10^{-6},$$
$$\mathcal{B}(B^+ \to \omega K^+) = (6.3 \pm 0.5 \pm 0.3) \times 10^{-6},$$
$$\mathcal{B}(B^0 \to \omega K^0) = (5.4 \pm 0.8 \pm 0.3) \times 10^{-6}.$$

For the charge asymmetries we find

$$\mathcal{A}_{\rm ch}(B^+ \to \eta\pi^+) = -0.08 \pm 0.10 \pm 0.01,$$
$$\mathcal{A}_{\rm ch}(B^+ \to \eta K^+) = -0.22 \pm 0.11 \pm 0.01,$$
$$\mathcal{A}_{\rm ch}(B^+ \to \eta'\pi^+) = 0.21 \pm 0.17 \pm 0.01,$$
$$\mathcal{A}_{\rm ch}(B^+ \to \eta' K^+) = 0.010 \pm 0.022 \pm 0.006,$$
$$\mathcal{A}_{\rm ch}(B^+ \to \omega\pi^+) = -0.02 \pm 0.08 \pm 0.01,$$
$$\mathcal{A}_{\rm ch}(B^+ \to \omega K^+) = -0.01 \pm 0.07 \pm 0.01.$$

The first error quoted is statistical and the second system-

atic. These results are generally consistent with published measurements [7–13] and supersede our previous ones [7–9]; for $\mathcal{B}(B^+ \to \eta K^+)$ we find a value about twice that of [10]. The theoretical estimates are in agreement with the data (though the data have been used in some predictions), but with greater uncertainty [1–3]. Approaches that fit all available data with a moderate number of model parameters have proved fruitful [4–6]. We find no clear evidence for direct *CP*-violation charge asymmetries in these decays. The world averages of the measurements of $\mathcal{A}_{\rm ch}$ for $B^+ \to \eta\pi^+$ ($B^+ \to \eta K^+$) are both negative and 2.3 (3.0) standard deviations from zero, while the predictions of [3] are positive, though with large errors.

We are grateful for the excellent luminosity and machine conditions provided by our PEP-II colleagues, and for the substantial dedicated effort from the computing organizations that support *BABAR*. The collaborating institutions wish to thank SLAC for its support and kind hospitality. This work is supported by DOE and NSF (USA), NSERC (Canada), CEA and CNRS-IN2P3 (France), BMBF and DFG (Germany), INFN (Italy), FOM (The Netherlands), NFR (Norway), MIST (Russia), MEC (Spain), and STFC (United Kingdom). Individuals have received support from the Marie Curie EIF (European Union) and the A. P. Sloan Foundation.

[1] M. Beneke and M. Neubert, Nucl. Phys. **B675**, 333 (2003) and references therein.
[2] M.-Z. Yang and Y.-D. Yang, Nucl. Phys. **B609**, 469 (2001); M. Beneke and M. Neubert, Nucl. Phys. **B651**, 225 (2003).
[3] A. Williamson and J. Zupan, Phys. Rev. D **74**, 014003 (2006).
[4] H. K. Fu *et al.*, Phys. Rev. D **69**, 074002 (2004).
[5] C.-W. Chiang *et al.*, Phys. Rev. D **70**, 034020 (2004).
[6] C.-W. Chiang, M. Gronau, and J. L. Rosner, Phys. Rev. D **68**, 074012 (2003); C.-W. Chiang *et al.*, Phys. Rev. D **69**, 034001 (2004).
[7] B. Aubert *et al.* (*BABAR* Collaboration), Phys. Rev. Lett. **95**, 131803 (2005).
[8] B. Aubert *et al.* (*BABAR* Collaboration), Phys. Rev. Lett. **94**, 191802 (2005).
[9] B. Aubert *et al.* (*BABAR* Collaboration), Phys. Rev. D **74**, 011106 (2006).
[10] P. Chang *et al.* (Belle Collaboration), Phys. Rev. D **75**, 071104(R) (2007).
[11] J. Schümann *et al.* (Belle Collaboration), Phys. Rev. Lett. **97**, 061802 (2006).
[12] C. H. Wang *et al.* (Belle Collaboration), Phys. Rev. D **70**, 012001 (2004).
[13] S. J. Richichi *et al.* (CLEO Collaboration), Phys. Rev. Lett. **85**, 520 (2000); C. P. Jessop *et al.*, Phys. Rev. Lett. **85**, 2881 (2000); S. Chen *et al.*, Phys. Rev. Lett. **85**, 525 (2000).
[14] B. Aubert *et al.* (*BABAR* Collaboration), Phys. Rev. D **74**, 051106 (2006).
[15] B. Aubert *et al.* (*BABAR* Collaboration), Phys. Rev. Lett. **98**, 031801 (2007).
[16] H. J. Lipkin, Phys. Lett. B **254**, 247 (1991).
[17] M. Bander, D. Silverman, and A. Soni, Phys. Rev. Lett. **43**, 242 (1979); S. Barshay, D. Rein, and L. M. Sehgal, Phys. Lett. B **259**, 475 (1991); A. S. Dighe, M. Gronau, and J. L. Rosner, Phys. Rev. Lett. **79**, 4333 (1997).
[18] G. Kramer, W. F. Palmer, and H. Simma, Nucl. Phys. **B428**, 77 (1994); A. Ali, G. Kramer, and C.-D. Lü, Phys. Rev. D **59**, 014005 (1998).
[19] A. Soni and D. A. Suprun, Phys. Rev. D **75**, 054006 (2007).
[20] A. Datta and D. London, Phys. Lett. B **595**, 453 (2004); M. Ciuchini *et al.*, Phys. Rev. D **67**, 075016 (2003).
[21] B. Aubert *et al.* (*BABAR* Collaboration), Nucl. Instrum. Methods Phys. Res., Sect. A **479**, 1 (2002).
[22] PEP-II Conceptual Design Report, SLAC-R-418, 1993.
[23] The *BABAR* detector Monte Carlo simulation is based on GEANT4: S. Agostinelli *et al.*, Nucl. Instrum. Methods Phys. Res., Sect. A **506**, 250 (2003).
[24] Y.-M. Yao *et al.* (Particle Data Group), J. Phys. G **33**, 1 (2006).
[25] B. Aubert *et al.* (*BABAR* Collaboration), Phys. Rev. D **70**, 032006 (2004).